ChemComm

Accepted Manuscript

ROYAL SOCIETY OF CHEMISTRY

rsc.li/chemcomm

View Article Online
DOI: 10.1039/C7CC04323F

Journal Name

COMMUNICATION

Synthesis of seminaphtho-phospha-fluorescein dyes based on the consecutive arylation of aryldichlorophosphines

Received 00th January 20xx,
Accepted 00th January 20xx

DOI: 10.1039/x0xx00000x

www.rsc.org/

Aiko Fukazawa,*[a] Junichi Usuba,[a] Raúl A. Adler,[b] and Shigehiro Yamaguchi*[ab]

Seminaphtho-phospha-fluorescein (SNAPF), a phosphine-oxide-containing unsymmetric fluorescein dye, was synthesized based on the consecutive arylation of $PhPCl_2$, followed by a Friedel-Crafts cyclization. The resulting SNAPF exhibited several attractive photophysical properties including an intense fluorescence in the NIR region and a large Stokes shift.

Water-soluble fluorescent dyes that exhibit light-absorption and fluorescence in the far-red to near-infrared (NIR) region have attracted increasing attention due to their application as fluorescent probes in bioimaging.[1] Among various types of small-molecule dyes, xanthene dyes, such as fluoresceins and rhodamines, represent dye skeletons that exhibit several advantages, including high solubility in aqueous media, large molar absorption coefficients, and high fluorescence quantum yields. However, the absorption and fluorescence wavelengths of the parent fluoresceins and rhodamines remain in the visible region. One promising strategy to induce bathochromically shifted absorption and fluorescence is the replacement of the endocyclic oxygen atom in the xanthene skeleton with another main-group element such as B (group 13),[2] Si and Ge (group 14),[3–5] P (group 15),[6–8] or S, Se, and Te (group 16).[9] These structural modifications afforded various intriguing fluorescent probes with characteristic properties.

Among these probes, phosphine-oxide-containing xanthene dyes, such as phospha-fluoresceins (POFs)[6] and phospha-rhodamines **1**,[7,8] are of particular importance (Figure 1a). The introduction of an electron-withdrawing P=O moiety decreases the energy levels of both the HOMO and LUMO, which results in a significant bathochromic shift of the absorption and emission bands to reach the NIR region. POF,

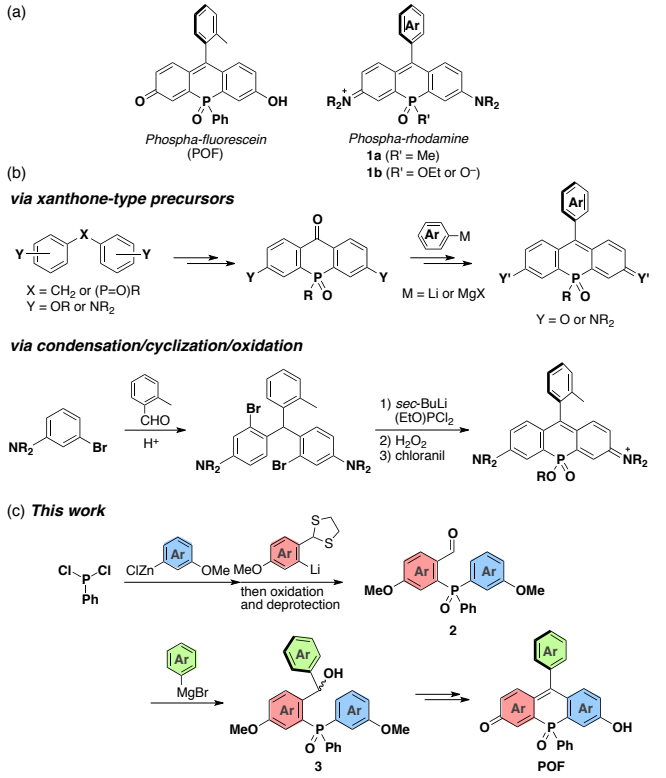

Fig. 1 (a) Molecular structures of phospha-xanthene dyes; (b) previously reported synthetic routes to phospha-xanthene dyes; (c) alternative synthetic route to POF explored in this study.

which we have recently reported, exhibited an intense far-red fluorescence (λ_{em} = 656 nm) and a high fluorescence quantum yield (0.33) in water at pH = 9. The P=O group also lowered the pK_a value to 5.7 relative to that of the parent fluorescein (~6.2), while retaining the characteristic pH-dependent character and high cell-membrane permeability.

Despite the potential utility of POFs, the lack of a versatile synthetic method has so far restrained a systematic fine-tuning of their structures. The synthetic methods reported to date can be divided into two sub-classes. One is based on phospha-xanthone precursors (Figure 1b; top), which allowed Wang and

[a] Department of Chemistry, Graduate School of Science and Integrated Research Consortium on Chemical Sciences (IRCCS), Nagoya University, Furo, Chikusa, Nagoya 464-8602, Japan. E-mail: yamaguchi@chem.nagoya-u.ac.jp.
[b] Institute of Transformative Bio-Molecules (WPI-ITbM), Nagoya University, Furo, Chikusa, Nagoya 464-8602, Japan.

† Electronic Supplementary Information (ESI) available: Experimental details, photophysical data, the results of X-ray crystallographic analyses and theoretical calculations. CCDC 1535531, 1535532, and 1535533. For ESI and crystallographic data in CIF or other electronic format see DOI: 10.1039/x0xx00000x

co-workers[7] and our group[6] to independently reported the synthesis of phospha-rhodamine **1a** and POF, respectively. However, the phospha-xanthone precursors themselves can so far only be accessed via laborious synthetic procedures, and the introduction of bulky aryl groups in the xanthones by nucleophilic addition of arylmetal reagents generally suffers from low yields despite the importance for highly emissive character.[10] The other method is based on the condensation of *m*-bromoanilines with benzaldehydes. Whereas Stains and co-workers have reported a relatively short synthesis of phospha-rhodamine **1b** using this approach (Figure 1b; bottom), this method is limited to the synthesis of rhodamine derivatives.[8] Moreover, the synthesis of unsymmetrically substituted phospha-xanthene dyes from either method is nontrivial.

In this context, a diversity-oriented synthesis of POFs that provides general access to even unsymmetrically substituted skeletons would be highly desirable for the systematic fine-tuning of these dyes. Our strategy to achieve this goal is based on the assembly of three aryl groups in a stepwise manner to generate arylhydroxymethyl-substituted phosphine oxides **3**, from which a Friedel-Crafts cyclization and a subsequent oxidation should furnish POFs[11] (Figure 1c). Herein, we report the details of this synthetic protocol. A seminaphtho-phospha-fluorescein thus synthesized as an example of unsymmetrically substituted POFs showed intriguing photophysical properties.

The first step of this synthesis involves the assembly of two aryl groups onto a phenylphosphine moiety starting from $PhPCl_2$. As an example of the key intermediate, we examined the synthesis of *o*-formyl-substituted triarylphosphine oxide **2a** (Scheme 1). Wittig and coworkers have reported that the reaction of $PhPCl_2$ with arylzinc reagents results in a selective monoarylation.[12] Accordingly, $PhPCl_2$ was initially treated with 1 equiv of *m*-methoxyphenylzinc chloride, before the second arylation was carried out with 2-dithiolanyl-5-methoxyphenyllithium, followed by oxidation with an aqueous H_2O_2 solution to yield unsymmetrically substituted triaryl-phosphine oxide **5a**. The mixture was subsequently treated with $AgNO_3$ to promote deprotection of the dithiolane moiety. All these procedures were conducted in one pot without isolation of any intermediates to yield **2a** in 47% over four steps from $PhPCl_2$.

Subsequently, the third aryl group was introduced. The nucleophilic addition of Grignard reagents, such as *o*-tolyl-magnesium bromide and 2,6-dimethylphenylmagnesium

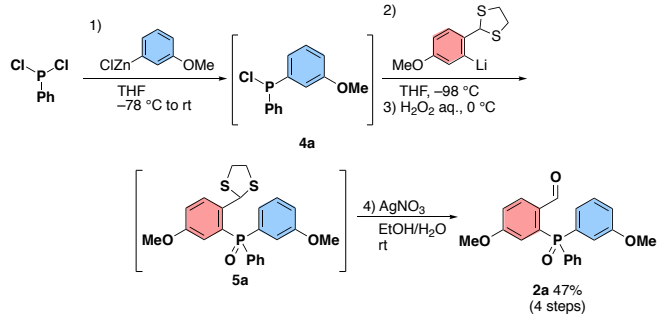

Scheme 1 Synthesis of unsymmetric triarylphosphine oxides via the consecutive arylation of $PhPCl_2$.

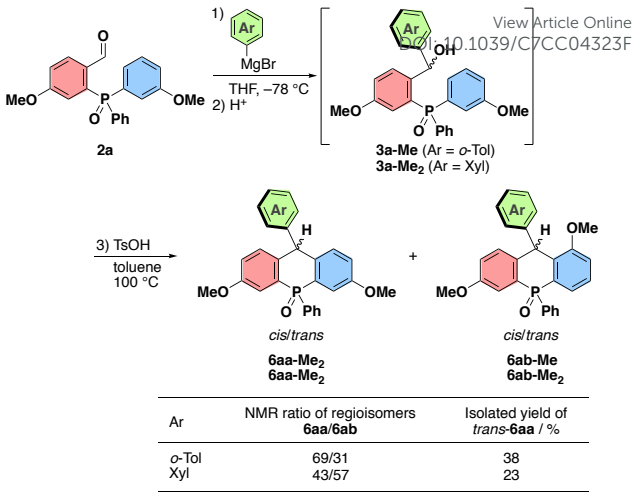

Ar	NMR ratio of regioisomers **6aa**/**6ab**	Isolated yield of *trans*-**6aa** / %
o-Tol	69/31	38
Xyl	43/57	23

Scheme 2 Synthesis of cyclic triarylphosphine oxides **6** from unsymmetric triarylphosphine oxides **2** by the nucleophilic addition and the intramolecular Friedel-Crafts cyclization of *o*-(hydroxymethyl)arylphosphine oxides.

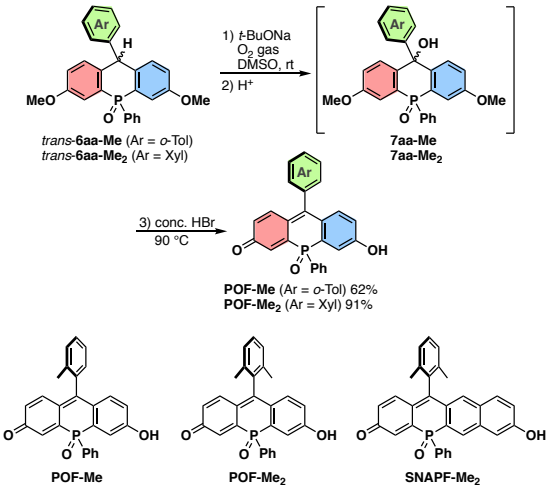

Scheme 3 Synthesis of POFs.

bromide, to **2a** cleanly afforded diastereoisomer mixtures of **3a-Me** and **3a-Me$_2$**, respectively. Without isolation of the products, a subsequent intramolecular Friedel-Crafts cyclization was conducted (Scheme 2). A screening of Lewis and Brønsted acids including $AlCl_3$, $Sc(OTf)_3$, TsOH, and camphorsulfonic acid showed that TsOH most effectively promoted the intramolecular Friedel-Crafts reaction. The cyclization produced two regioisomers (**6aa** and **6ab**), both of which were obtained as a mixture of *cis*/*trans* isomers with respect to the orientation of the C–Ar and P–Ph bonds.[§] Purification by column chromatography afforded *trans*-**6aa-Me** and *trans*-**6aa-Me$_2$** in 38% and 23% yield, respectively.

Finally, the oxidation of *trans*-**6aa-Me** and *trans*-**6aa-Me$_2$** with *t*-BuONa under an atmosphere of oxygen afforded the corresponding benzylic alcohols **7aa-Me** and **7aa-Me$_2$** (Scheme 3). Further treatment with HBr furnished POF-Me and POF-Me_2 in good to excellent yields.

In principle, this synthetic method should be applicable to various unsymmetric POF analogues using appropriate

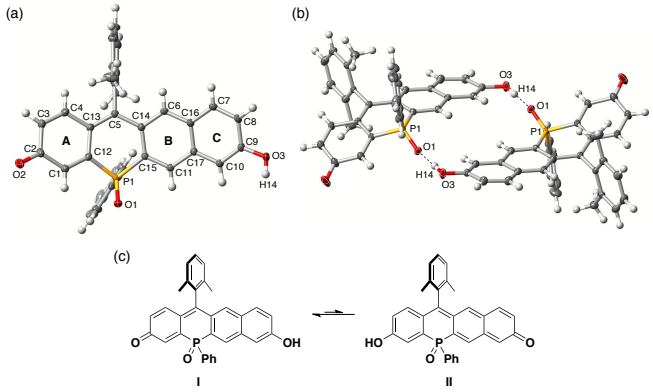

Fig. 2 X-ray crystal structures of (a) SNAPF-Me_2 and (b) the corresponding dimer through hydrogen bonds (thermal ellipsoids set to 50% probability; only selected atoms are labeled) and (c) tautomerization of SNAPF-Me_2.

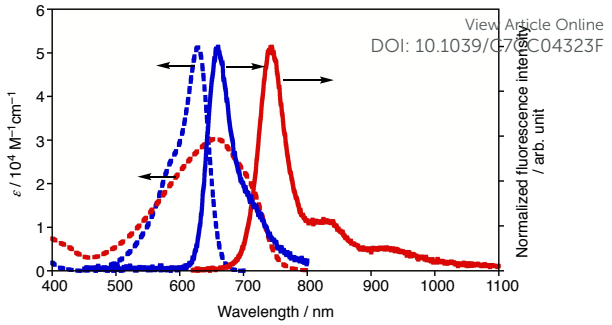

Fig. 3 UV-vis-NIR absorption (dashed lines) and fluorescence spectra (solid lines) for POF-Me_2 (blue) and SNAPF-Me_2 (red) in pH-buffer solutions (pH = 9; 0.1 M Na_2CO_3/$NaHCO_3$) containing 1% DMSO.

arylmetal reagents. As a proof-of-concept study, a seminaphtho-phospha-fluorescein (hereafter abbreviated to SNAPF-Me_2) was synthesized using 7-methoxy-2-naphthylzinc chloride as a nucleophile in the first step (Schemes 1 and S2–4), which afforded deep red crystals of SNAPF-Me_2.

A single-crystal X-ray diffraction analysis revealed the characteristic features of unsymmetrically π-extended SNAPF-Me_2 (Figs. 2a,b). Similar to POF, the π-conjugated skeleton in SNAPF-Me_2 adopts a slightly bent structure due to an envelope-like geometry of the phosphorus-containing six-membered ring. The π-skeleton shows pronounced bond alternation, i.e., the C9–O3 bond [1.351(2) Å] is substantially longer than the C2–O2 bond [1.239(2) Å]. The six-membered ring C1–C2–C3–C4–C13–C12 exhibits a higher degree of bond alternation than the six-membered rings in the naphthalene moiety (C6–C16-C17–C11–C15–C14 and C7–C8–C9–C10–C17–C16). Moreover, SNAPF-Me_2 forms dimers in the crystal lattice, evident from the short interatomic distance between the O1 and O3 atoms (2.653 Å) in adjacent molecules, which indicates the presence of intermolecular hydrogen bonds between a phenolic proton on the naphthalene moiety and a phosphine oxide moiety.[13] These structural features demonstrate the predominant contribution of the benzoquinone/naphthol tautomer **I** relative to the phenol/naphthoquinone tautomer **II** (Fig. 2c).

DFT calculations at the B3LYP/6-31+G* level of theory revealed that tautomer **I** is by 6.23 kcal mol^{-1} more stable than **II**. This difference results most likely from the larger aromatic stabilization gained in **I** compared to **II**, which is due to the fact that only one benzene ring retains aromaticity in tautomer **II**, while two benzene rings in the naphthalene moiety of **I** can retain aromaticity. An NMR analysis of SNAPF-Me_2 suggested that tautomer **I** is also the dominant species in dilute solution at ambient temperature (Figs. S42–S48).

The photophysical properties of POF-Me_2 and SNAPF-Me_2 were investigated in aqueous buffer solutions containing 1% DMSO as a co-solvent (Fig. 3, Table 1, and Figs. S9–12). Both POF-Me_2 and SNAPF-Me_2 exhibited pH-dependent absorption spectra similar to other fluoresceins. In the absorption spectrum of POF-Me_2, the absorption band at λ_{abs} = 488 nm diminished upon increasing the pH value of the solution from 3 to 11, and a new broad band emerged at λ_{abs} = 628 nm with an isosbestic point at 537 nm (Fig. S9). This bathochromically shifted absorption band under basic conditions was ascribed to an anionic form of POF-Me_2. The photophysical properties of POF-Me_2 are almost identical to those of the previously reported POF-Me,[6] indicating that the increased steric demand at the 9-position does not affect the photophysical properties of POFs.

In comparison with POF-Me_2, SNAPF-Me_2 exhibits a more pronounced bathochromic shift of the absorption band at λ_{abs} = 499 nm (pH = 3) to λ_{abs} = 654 nm (pH = 9), with an isosbestic point at 550 nm (Fig. 3, Table 1, and Fig. S11). This difference was attributed to the expansion of the π-conjugation in SNAPF-Me_2 relative to POF-Me_2. Notably, the π-expansion in SNAPF-Me_2 also affects the pK_a value. Based on a plot of the absorbance change at λ_{abs} = 654 nm, the pK_a value of SNAPF-Me_2 was determined to be 7.7, which was much higher than that of POF-Me_2 (5.7) (Fig. S13). Considering the results of the X-ray crystallographic and the NMR analyses, SNAPF-Me_2 exhibits a certain naphthol character, which should be responsible for the increased pK_a value.

Under basic conditions, deprotonated SNAPF-Me_2 exhibited a sharp fluorescence band at λ_{em} = 744 nm (Fig. 3), which is by 88 nm bathochromically shifted relative to that of POF-Me_2 (λ_{em} = 656 nm).[§§] The Stokes shift of SNAPF-Me_2 (1850 cm^{-1}) is substantially larger than that of POF-Me_2 (~ 700 cm^{-1}), indicative of a more pronounced charge-transfer character of the lowest-energy excited singlet state (S_1) in SNAPF-Me_2, where the unsymmetric structure plays a crucial role. Geometry optimizations based on (TD-)DFT calculations for the model compounds SNAPF-Me and POF-Me in S_0 and S_1 demonstrated that SNAPF-Me undergoes a large structural relaxation from the Frank-Condon state in S_1 to form a more unsymmetric structure compared to the ground-state structure, with increased and decreased bond alternation in the benzene and naphthalene moieties, respectively (Fig. S7). This behavior stands in stark contrast to that of POF-Me, which undergoes a symmetric structural change in S_1 with a slightly increased bond alternation in both benzene rings (Fig. S6).

A comparison with known oxygen-containing seminaphtho-fluoresceins (hereafter abbreviated as SNAFs; Fig. 4)[14,15]

Table 1 Comparison of the photophysical properties and pK_a values of SNAPF and relevant fluorescein derivatives

Compound	Absorption		Fluorescence		Stokes shift / cm^{-1}	pK_a
	λ_{abs} / nm	ε / 10^4 M^{-1} cm^{-1}	λ_{em} / nm	Φ_{FL}		
SNAPF-Me_2[a]	654	2.87	744	0.03[b]	1850	7.7
POF-Me_2[a]	628	5.41	656	0.32[b]	680	5.7
POF-Me[a,c]	627	5.13	656	0.33[b]	710	5.7
SNAF-H[d]	536	1.40	733	n.d.	5010	8.2
SNAF-COOH[e]	536	2.90	732	0.0024	5000	–

[a]pH = 9 in an aqueous pH-buffer solution containing 0.1 M Na_2CO_3/$NaHCO_3$. [b]Absolute fluorescence quantum yields were determined using an integrating sphere system. [c]Ref. 6. [d]Ref. 14. [e]Ref. 15.

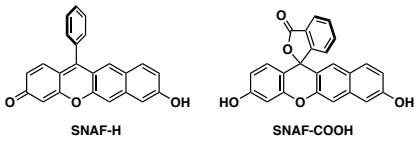

Fig. 4 Chemical structures of seminaphtho-fluorescein SNAF-H[13] and SNAF-COOH[14].

highlights the characteristic features of SNAPF as a scaffold for NIR-emitting fluorescent probes. A significant difference between SNAFs and SNAPFs is evident in their absorption spectra, where SNAPF exhibits a bathochromically shifted maximum wavelength by 118 nm compared to SNAF-H (λ_{abs} = 536 nm) in their deprotonated forms. SNAPF moreover exhibits a bathochromically shifted emission wavelength by 11 nm than SNAF-H (λ_{em} = 733 nm), while the fluorescence quantum yield of e.g. SNAPF-Me_2 (Φ_{FL} = 0.03) remains by one order of magnitude higher than that of e.g. SNAF-COOH (Φ_{FL} = 0.0024). Furthermore, the pK_a value of SNAPF-Me_2 (7.7) is lower than that of SNAF-H (8.2), which is most likely due to the electron-withdrawing character of the phosphine oxide moiety. In light of the fact that the pH value of cytosol in living animal cells ranges from 6.8–7.4, SNAPFs should thus represent potentially suitable materials for pH-responsive fluorophores for bioimaging.

In summary, we have established a robust synthetic route to phospha-fluorescein dyes based on the consecutive arylation of $PhPCl_2$. This protocol provides not only facile access to POFs with various bulky aryl groups at the 9-position, but also to unsymmetric POF analogues, which are difficult to synthesize using conventional methods. As an example of the latter compound class, SNAPF was synthesized. Compared to the symmetrically substituted POFs, SNAPF exhibited several attractive properties, including a high pK_a value, red-shifted absorption, and NIR fluorescence, as well as a large Stokes shift. This SNAPF may have potential utility as an NIR fluorescence dye. Further structural modifications of POFs directed towards applications in bioimaging are currently in progress in our laboratory.

The authors would like to thank Prof. T. Sasamori (Nagoya City Univ.), and Drs. M. Hirai and H. Oshima (Nagoya Univ.) for their help for the single-crystal X-ray diffraction analysis. This work was partly supported by the JSPS KAKENHI grant 16K13949. Further financial supports from the Nagase Science and Technology Foundation and the Naito Foundation are gratefully acknowledged. ITbM is supported by the World Premier International Research Center Initiative (WPI, Japan).

View Article Online DOI: 10.1039/C7CC04775

Notes and references

§ Their isomer ratios were determined based on the integration ratio in the ^{31}P NMR spectrum; for details, see ESI.
§§ At lower pH values, the emission spectrum of SNAPF-Me_2 is dominated by the deprotonated form, even though a second emission band at λ_{em} = 655 nm can be assigned to the emission from the neutral form (Fig. S12); for details, see: ESI.

1 For recent accounts and reviews, see: (a) S. A. Hilderbrand and R. Weissleder, *Curr. Opin. Chem. Biol.*, 2010, **14**, 71. (b) S. Luo, E. Zhang, Y. Su, T. Cheng and C. Shi, *Biomaterials*, 2011, **32**, 7127. (c) V. J. Pansare, S. Hejazi, W. J. Faenza and R. K. Prud'homme, *Chem. Mater.*, 2012, **24**, 812.
2 N. Shimomura, Y. Egawa, R. Miki, T. Fujihara, Y. Ishimaru and T. Seki, *Org. Biomol. Chem.*, 2016, **14**, 10031.
3 For a recent review, see: Y. Kushida, T. Nagano and K. Hanaoka, *Analyst*, 2014, **140**, 685.
4 T. Egawa, Y. Koide, K. Hanaoka, T. Komatsu, T. Terai and T. Nagano, *Chem. Commun.*, 2011, **47**, 4162.
5 (a) M. Fu, Y. Xiao, X. Qian, D. Zhao and Y. Xu, *Chem. Commun.* 2008, 1780; (b) Y. Koide, Y. Urano, K. Hanaoka, T. Terai and T. Nagano, *ACS Chem. Biol.*, 2011, **6**, 600; (c) Y. Koide, Y. Urano, K. Hanaoka, T. Terai and T. Nagano, *J. Am. Chem. Soc.*, 2011, **133**, 5680; (d) T. Egawa, K. Hanaoka, Y. Koide, S. Ujita, N. Takahashi, Y. Ikegaya, N. Matsuki, T. Terai, T. Ueno, T. Komatsu and T. Nagano, *J. Am. Chem. Soc.*, 2011, **133**, 14157; (e) Y. Koide, T. Urano, K. Hanaoka, W. Piao, M. Kusakabe, N. Saito, T. Terai, T. Okabe and T. Nagano, *J. Am. Chem. Soc.*, 2012, **134**, 5029.
6 A. Fukazawa, S. Suda, M. Taki, E. Yamaguchi, M. Grzybowski, Y. Sato, T. Higashiyama and S. Yamaguchi, *Chem. Commun.*, 2015, **52**, 1120.
7 X. Chai, X. Cui, B. Wang, F. Yang, Y. Cai, Q. Wu and T. Wang, *Chem.-Eur. J.*, 2015, **21**, 16754.
8 X. Zhou, R. Lai, J. Beck, H. Li and C. Stains, *Chem. Commun.*, 2016, **52**, 12290.
9 (a) M. R. Detty, P. N. Prasad, D. J. Donnelly, T. Ohulchanskyy, S. L. Gibson and R. Hilf, *Bioorg. Med. Chem.,* 2004, **12**, 2537; (b) B. Calitree, D. J. Donnelly, J. J. Holt, M. K. Gannon, C. L. Nygren, D. K. Sukumaran, J. Autschbach and M. R. Detty, *Organometallics*, 2007, **26**, 6248; (c) M. W. Kryman, G. A. Schamerhorn, K. Yung, B. Sathyamoorthy, D. K. Sukumaran, T. Y. Ohulchanskyy, J. B. Benedict and M. R. Detty, *Organometallics*, 2013, **32**, 4321; (d) M. W. Kryman, G. A. Schamerhorn, J. E. Hill, B. D. Calitree, T. Y. Ohulchanskyy and M. R. Detty, *Organometallics*, 2014, **33**, 2628.
10 Y. Ueno, M. Kamiya, K. Kanda, T. Ueno, K. Hirose and T. Nagano, *J. Am. Chem. Soc.* 2005, **127**, 4888.
11 Z. Lei, X. Li, Y. Li, X. Luo, M. Zhou and Y. Yang, *J. Org. Chem.* 2015, **80**, 11538.
12 G. Wittig, H. Braun and H. Cristau, *Liebigs Ann. Chem.*, 1971, **751**, 17.
13 T. Steiner, *Angew. Chem. Int. Ed.*, 2002, **41**, 48.
14 Y. Yang, M. Lowry, X. Xu, I. O. Escobedo, M. Sibrian-Vazquez, L. Wong, C. M. Schowalter, T. J. Jensen, F. R. Fronczek, I. M. Warner and R. M. Strongin, *Proc. Nat. Acad. Sci.*, 2008, **105**, 8829.
15 E. Azuma, N. Nakamura, K. Kuramochi, T. Sasamori, N. Tokitoh, I. Sagami and K. Tsubaki, *J. Org. Chem*, 2012, **77**, 3492.

View Article Online
DOI: 10.1039/C7CC04323F

Journal Name

COMMUNICATION